Study on the effect of fuels on phase formation and morphology of combustion derived α-Al₂O₃ and NiO nanomaterials

R. S. Raveendra[2], P. A. Prashanth[1*], B. M. Nagabhushana[3]

[1]*Research Centre, Department of Chemistry, SVIT, Bengaluru 560064, India*
[2]*Research & Development Centre, Bharathiar University, Coimbatore 641046, India*
[3]*Department of Chemistry, M.S. Ramaiah Institute of Technology, Bengaluru 560054, India*

[*]Corresponding author. Tel: (+91) 9663313591; E-mail: prsnthmysore@gmail.com

ABSTRACT

In this study we present an effect of glycine and urea fuels on the phase formation and morphology of the α-Al₂O₃ and NiO nanomaterials. Materials were synthesized using facile solution combustion method at temperature 500 °C ± 10 °C. The synthesized products were characterized by various analytical techniques. PXRD results of α-Al₂O₃ confirm that the hexagonal phase is best represented using urea as a fuel compared to glycine. FE-SEM micrographs observed with urea are like flake like structure whereas with glycine net like porous structure is observed. TEM micrographs show the well crystalline nature of the nanomaterials. Large mismatching was observed in the FTIR spectra of synthesized materials using urea and glycine fuels with respect to the OH and metal to oxygen vibrational frequencies. PXRD results of NiO confirm that the cubic structure is obtained with urea fuel without any secondary phases, whereas with glycine a small peak of Ni was observed at 2θ = 44.5°. FE-SEM micrographs NiO with urea represents spherical like structure whereas large number of voids with porous structure was observed with glycine. The results of the study show that the fuels used for the synthesis of nanomaterials have a great effect on phase formation and morphology. Copyright © 2016 VBRI Press.

Keywords: Morphology; hexagonal; porous; glycine; solution combustion.

Introduction

α-Al₂O₃ (Corundum) represents a ceramic material with important technical and industrial importance [1]. Mainly this is due to its versatile features, such as: exceptional mechanical strength at room temperature and high temperature, inflexibility and abrasion resistance, high melting point, chemical inertness, thermal shock resistance, large band-gap and so on. Such unique properties made corundum one of the most commonly used materials for various applications: cutting tools [2], electronic components and substrates [3], abrasives, bioceramics [4], refractory materials, composite materials [5], spark-plugs, ballistic armours [6], thermoluminescent dosimeters [7], photoluminescent material [8], cytotoxic agent [9] and so on.

Various polymorphs of alumina were synthesized and reported for different applications. A mixture of fuel approach has been employed to rapidly synthesize single phase polycrystalline powders of γ- alumina a mixture of urea and glycine as fuel in a solution combustion method [10]. The size relationships between the crystallite and the related agglomerate size for θ-and α-Al₂O₃ particles during θ→α -Al₂O₃ phase transformation of alumina powders has been examined using chemical precipitation methods [11]. Urea was used as a chelating agent for the single-stage synthesis of fine α-Al₂O₃ powders using solution combustion method [12].

Magnetic metal nanoparticles, such as nickel, cobalt and iron, have attracted significant awareness in the past 20 years because of unique fundamental properties involved and technological applications in various fields such as multilayer ceramic capacitors (MLCs), magnetic storage media and so on [13]. NiO nanoparticles are of great concern as model systems for study of magnetic interactions and superparamagnetism which are influenced by nanostructure parameters which in turn depend on synthesis strategies. The study of small nano size particles is of much present interest due to the improved properties bulk materials show when the crystal size is reduced [14]. The effect of different fuels has a great influence on the phase formation and morphology of the nanoparticles. In the current article we present the synthesis of α- Al₂O₃ and NiO nanomaterials by low temperature solution combustion method using urea and glycine as fuels and studied phase formation morphological effect.

The advantage of this study is that the fuels used contains amine group which helps in the combustion of the precursor materials at lower temperature. It is understood that the urea containing two amine groups gives a better morphology compare to glycine containing zwitter ion. However the combustion synthesis method is less time

consuming and simpler compared to any other methods available in the literature.

## Experimental

Materials/Chemicals

All the chemicals and reagents used in this study were of analytical grade. Commercially available pure aluminium nitrate (Al(NO$_3$)$_3$ 9.H$_2$O, 99 % Merck), urea (CO(NH$_2$)$_2$ 99 % Merck), glycine (C$_2$H$_5$NO$_2$ 99 % Merck), nickel nitrate (Ni(NO$_3$)$_2$ 6.H$_2$O, 99 % Merck), double distilled water were used without any further purification.

Synthesis of α-Al$_2$O$_3$ and NiO nanomaterials

To synthesize α-Al$_2$O$_3$ and NiO nanomaterials solution combustion method was used [15 -17]. The stoichiometry of the redox mixture for combustion is calculated based on the total oxidizing and reducing valencies of the oxidizer and the fuel using the concept of propellant chemistry. The amounts of metal nitrates to fuel ratios for the synthesis of the nanoparticles are based on the following equation.

$$Oxidizer\,/fuel\,ratio = \frac{\Sigma all\ oxidizing\ and\ reducing\ elements\ in\ oxidizer}{(-1)\ \Sigma oxidizing\ and\ reducing\ elements\ in\ fuel} \quad (1)$$

Fuel type and fuel/aluminium nitrate molar ratio proved to be of great importance during the preparation of α-Al$_2$O$_3$ powders [18]. Al(NO$_3$)$_3$ 9H$_2$O was used as oxidizer, CO(NH$_2$)$_2$ and C$_2$H$_5$NO$_2$ were used as fuels, precursor mixture was magnetically stirred well in a crystalline dish for about 30 min with distilled water to get homogeneous mixture, then it was introduced into the pre-heated muffle furnace at 500 ± 10 °C. The solution was boiled and the resulted viscous liquid catches fire, auto ignited with flames on the surface which rapidly proceeded throughout the entire volume forming a white powdered product. The overall reaction of with urea can be written as,

$$2\ Al\ (NO_3)_3 + 3\ CO\ (NH_2)_2 \rightarrow Al_2O_3 + 6\ H_2O + 6\ N_2 + 3\ CO_2 \quad (2)$$
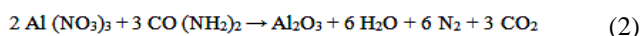
To synthesize NiO nanoparticles (Ni(NO$_3$)$_2$ 6H$_2$O was used as oxidizer, CO(NH$_2$)$_2$ and C$_2$H$_5$NO$_2$ were used as fuels, precursor mixture was stirred well using magnetic stirrer for about 30 min with distilled water. Then it was placed in a pre-heated muffle furnace at 500 ± 10 °C. Initially the solution was boiled and then resulted viscous liquid catches fire, auto ignited with flames on the entire surface forming a green powdered product. The overall reaction with urea fuel can be written as,

$$3\ Ni\ (NO_3)_2 + 5\ CO\ (NH_2)_2 \rightarrow 3\ NiO + 8\ N_2 + 5\ CO_2 + 10\ H_2O \quad (3)$$
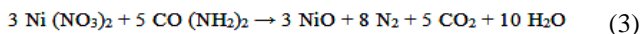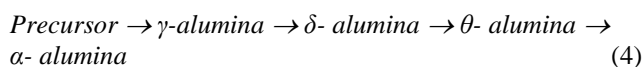
Characterizations

To find out the phase formation, nanomaterials were characterized by PXRD. Powder X- ray diffraction patterns were recorded on a Shimadzu XRD-700 X-ray Diffractometer with CuKα radiation with diffraction angle range 2θ = 20° to 80° operating at 40 kV and 30 mA. To study the crystallite size and morphology of the product, TEM analysis was performed on a Hitachi H-8100 (accelerating voltage upto 200 KV, LaB6 Filament). FE-SEM performed on a ZEISS ULTRA 55 scanning electron microscope. The FT-IR studies have been recorded on a Perkin Elmer Spectrometer (Spectrum 1000) with KBr pellet method in the range of 400-4000 cm^{-1}.

Results and discussion

Powder X-Ray diffraction studies

Previous studies reported that the formation of the crystalline phase of α-Al$_2$O$_3$ passes by means of thermal treatment through the following series of polymorphic phase transformation before final conversion to the thermodynamically stable phase α-Al$_2$O$_3$ polymorph (Corundum) [11].

$$Precursor \rightarrow \gamma\text{-}alumina \rightarrow \delta\text{-}alumina \rightarrow \theta\text{-}alumina \rightarrow \alpha\text{-}alumina \quad (4)$$

The mechanism for the α-Al$_2$O$_3$ phase transformation through precursor has been postulated and discussed previously and confirmed that α-Al$_2$O$_3$ was formed through the nucleation and growth process [19].

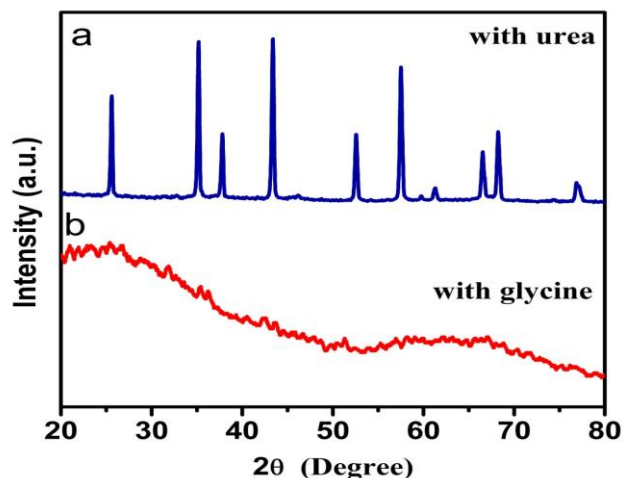**Fig. 1.** (a-b) PXRD patterns of α-Al$_2$O$_3$ with urea and glycine.

The PXRD results were examined with Crystallographica Search-Match (CSM). The PXRD of sample show the crystalline nature of sample having hexagonal structure (matched with ICDD card number 46-1212 with space group R-3c (No-167)), and cell parameters a = 4.7587 Å, b = 4.7587 Å, c = 12.9929 Å. All the diffraction peaks can be indexed to (0 1 2), (1 0 4), (1 1 0), (0 0 6) (1 1 3), (2 0 2), (0 2 4), (1 1 6), (2 1 1), (1 2 2), (0 1 8), (2 1 4), (3 0 0), (1 2 5) and (2 0 8) reflections. **Fig. 1(a, b)** shows the powder X-ray diffraction patterns of α-Al$_2$O$_3$ with urea and glycine respectively. The crystallite size is calculated from the full width at half maximum (FWHM (β)) of the diffraction peaks using Debye- Scherer's method [20] using the following equation,

$$d = \frac{k\lambda}{\beta cos\theta} \quad (5)$$

where, 'd' is the average crystalline dimension perpendicular to the reflecting phases, 'λ' is the X-ray wavelength, 'k' is Scherer's constant (0.92), 'β' is the full width at half maximum (FWHM) intensity of a Bragg reflection excluding instrumental broadening and 'θ' is the

Bragg's angle. The calculated average crystallite size of the α-Al$_2$O$_3$ with urea is found in the range of 20-30 nm.
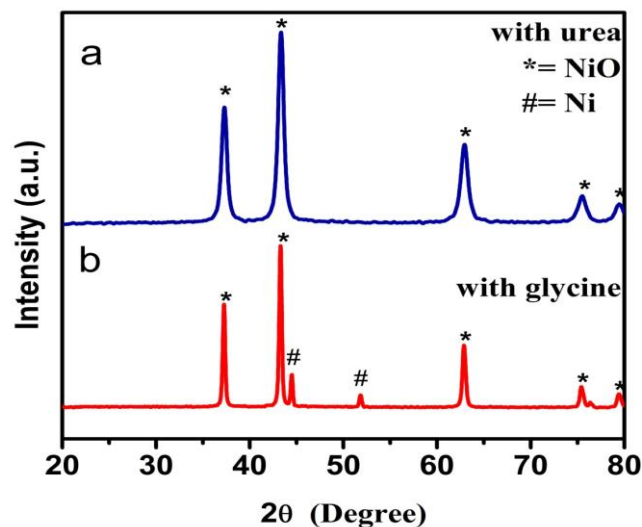

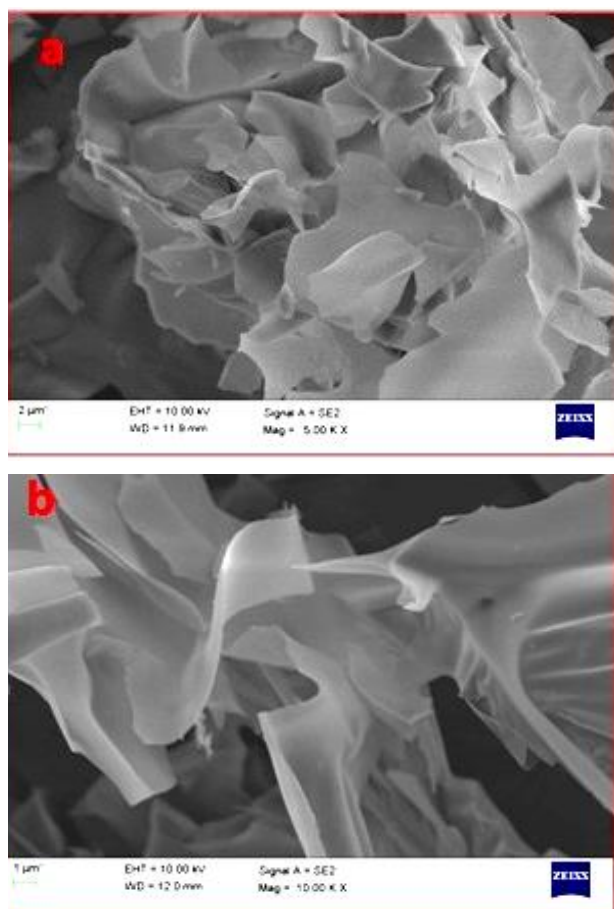**Fig. 2.** (a-b) PXRD patterns of NiO with urea and glycine.

Fig. 3. (a-b) FE-SEM micrographs of α-Al$_2$O$_3$ with urea.

The effect of fuel

The effect of fuel type on the phase formation of α-Al$_2$O$_3$ was studied. In the case of urea, the combustion process was very energetic, characterized by the incandescence of raw material mixture and the presence of bright flames. In the case of glycine, there was no sign of a visible combustion reaction; instead, reddish-brown gases could be seen, indicating the decomposition of aluminium nitrate [1]. The preparation of α-Al$_2$O$_3$ with the glycine fuel requires extra oxidizer (NH$_4$NO$_3$) than the stoichiometry [15].

The PXRD (**Fig. 2a**) of NiO with urea show the crystalline nature having cubic structure (matched with ICDD card number 89-7130 with space group Fm-3m (No-225)), and cell parameters a=b=c= 4.1944 Å. All the diffraction peaks can be indexed to (1 1 1), (2 0 0), (2 2 0), (3 1 1) and (2 2 2) reflections. The broadening of the reflections clearly indicates the inherent nature of nanocrystals. The calculated average crystallite size of the NiO with urea using Debye- Scherer's method is found in the range of 13-15 nm.

With glycine (**Fig. 2b**) a small peak of Ni was observed at 2θ=44.5°. This may be due to reduction of nickel nitrate to nickel because glycine being strong reducing than the urea reduces nickel nitrate to nickel.
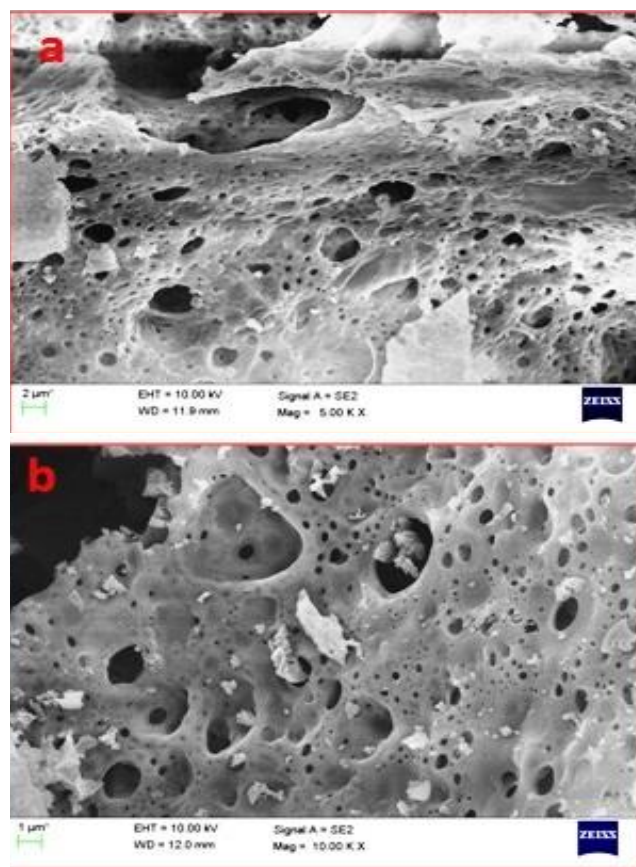

Fig. 4. (a-b) FE-SEM micrographs of α-Al$_2$O$_3$ with glycine.

Morphological analyses

The morphology of synthesized α-Al$_2$O$_3$ and NiO nanomaterials obtained with urea significantly differs from that of α-Al$_2$O$_3$ and NiO obtained with glycine. **Fig. 3(a-b)** shows FE-SEM images of α-Al$_2$O$_3$ with urea which is flake like structured, aggregates with urea and denser, larger and more durable. **Fig. 4(a-b)** shows FE-SEM images of α-Al$_2$O$_3$ with glycine which is more porous, friable structure. This may be due to the release of large number of gaseous products with glycine than with urea [12].
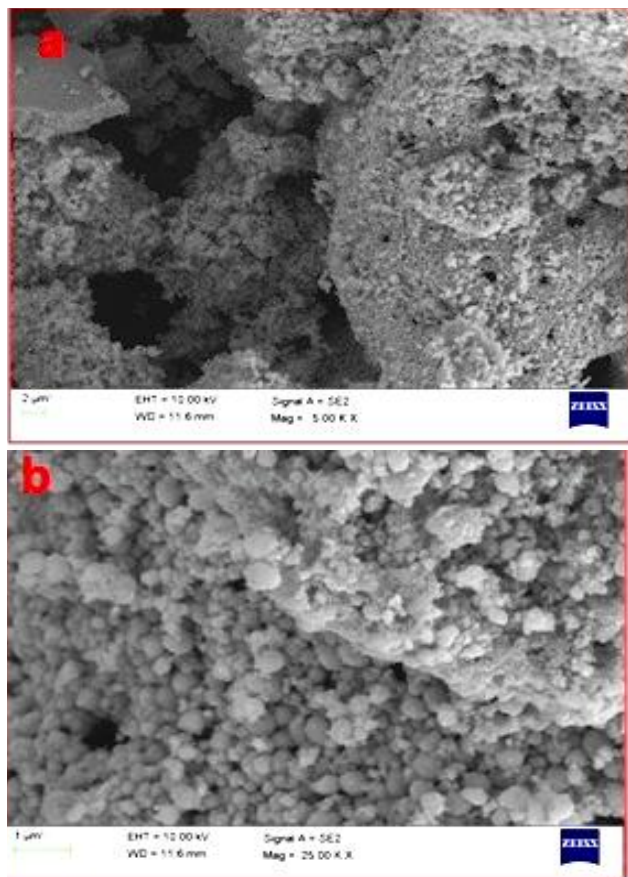
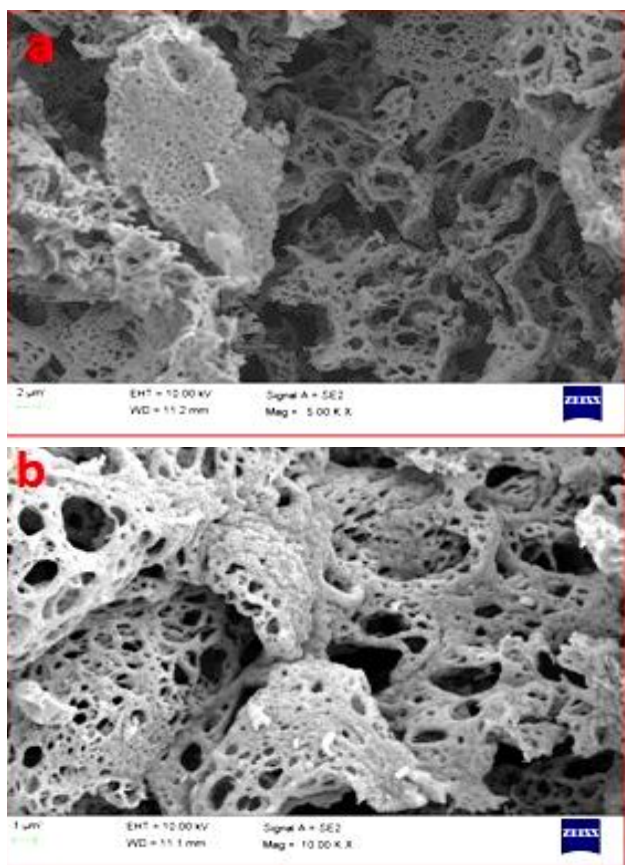**Fig. 5.** (a-b) FE-SEM micrographs of NiO with urea.

Fig. 6. (a-b) FE-SEM micrographs of NiO with glycine.

The morphology of prepared NiO nanoparticles was investigated using FE-SEM. **Fig. 5**(**a-b**) shows FE-SEM images NiO with urea. It revealed that the morphology of the NiO nanoparticles is a spherical shape and has uniform distribution. **Fig. 6**(**a-b**) shows FE-SEM images NiO with glycine which is more porous and net like structured.

The proof for the crystallinity of both nanomaterials was obtained by TEM investigations. The TEM method is better than X-ray line broadening in that it is direct and less likely to be affected by experimental errors and or other properties of the particles such as internal strain or distribution in the size of the lattice parameter. TEM patterns of α-Al_2O_3 with urea (**Fig. 7**) and NiO with urea (**Fig. 8**) shows that the particles obtained are in nano regime and have highly crystalline and average particle size ~ 15 nm.
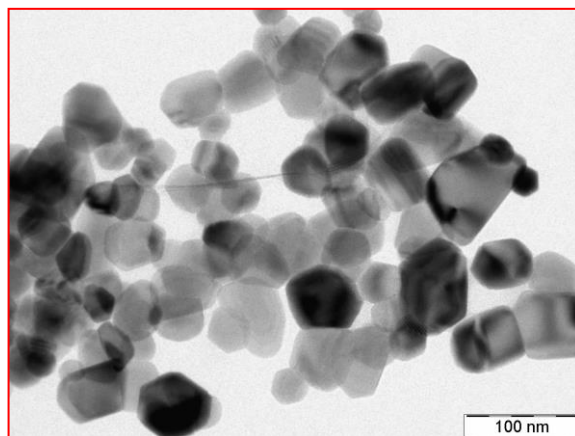
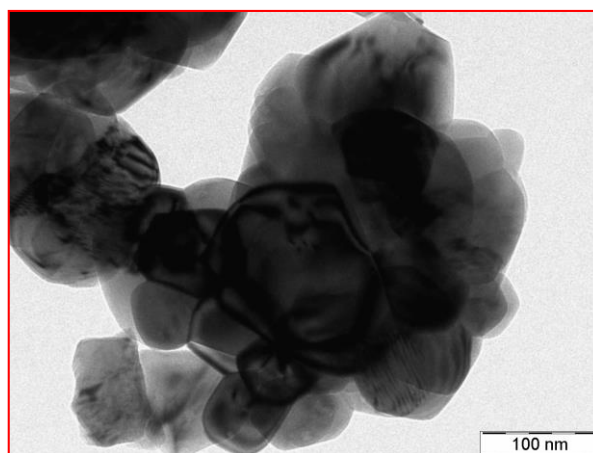**Fig. 7.** TEM of α-Al_2O_3 with urea**.**

Fig. 8. TEM of NiO with urea.

FT-IR spectroscopic studies

Fig. 9 (**a, b**) represents FT-IR spectrum of the α-Al_2O_3 with urea and glycine recorded to define the vibrational frequency of Metal–Oxygen and other bonds related to impurities present in the α-Al_2O_3 nanomaterial. It can be seen that no impurity peaks corresponding to the organic matter was observed. Strong absorption bands at 576 cm^{-1} (with urea) and 780 cm^{-1} (with glycine) can be assigned to the stretching vibration of Al–O bond. There is no much difference between spectrum with urea and glycine.
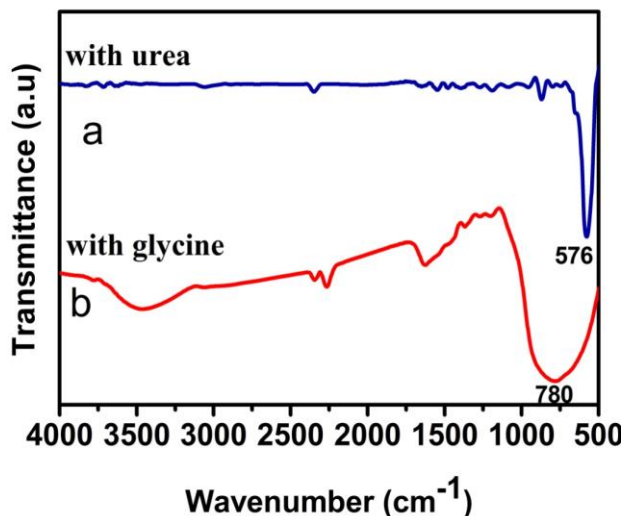
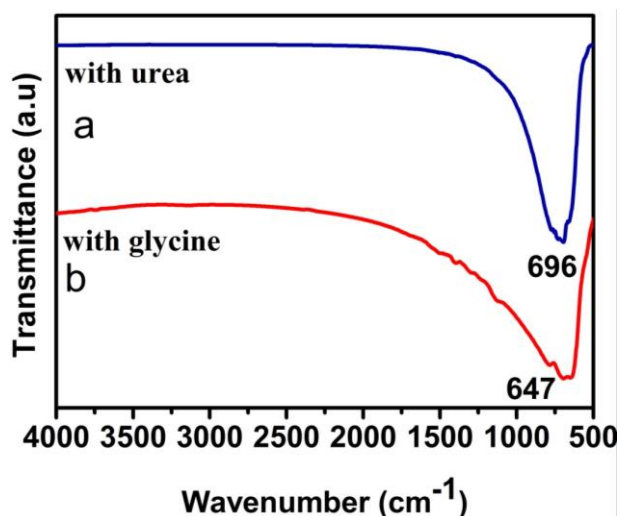**Fig. 9** (a-b) FT-IR spectrum of α-Al$_2$O$_3$ with urea and glycine.

Fig. 10. (a-b) FT-IR spectrum of NiO with urea and glycine.

Fig. 10(**a-b**) represents FT-IR spectrum of the NiO with urea and glycine recorded to define the vibrational frequency of Metal–Oxygen and other bonds related to impurities present in the NiO nanoparticles. Strong absorption bands at 696 cm^{-1} (with urea) and 647 cm^{-1} (with glycine) can be assigned to the stretching vibration of Ni–O bond.

Conclusion

A different fuels approach has been employed to synthesize α-Al$_2$O$_3$ and NiO nanomaterials using a urea and glycine as fuels in a solution combustion method. The use of urea best describe the formation of single phase without any impurities at low temperature compared to glycine. Glycine reduces the exothermicity of combustion reaction and acting as both complexing agent and fuel.

Reference

1. Ianos R.; Lazau I.; Pacurariu C.; *J. Mater. Sci.* **2009**, *44*, 1016.
   DOI: 10.1007/s10853-008-3226-5
2. Volceanov E.; Volceanov A.; Stoleriu S.; *J. Eur. Ceram Soc.* **2007**, *27*, 759.
   DOI: 10.1016/j.jeurceramsoc.2006.04.005
3. Menecier S.; Jarrige J.; Labbe J.C.; *J. Eur. Ceram. Soc.* **2007**, *27*, 851.
   DOI: 10.1016/j.jeurceramsoc.2006.04.036
4. Gitknecht D.; Chevalier J.; Garnier V.; *J. Eur. Ceram. Soc.*, **2007**, *27*, 1547.
   DOI: 10.1016/j.jeurceramsoc.2006.04.123
5. Ulyanova T.M.; Titova L.V.; Krutko N.P.; *Glass Ceram.,* **2002**, *59*, 279.
   DOI: 10.1023/A: 1020904001597
6. Badmos A.Y.; Ivey D.G.; *J. Mater. Sci.,* **2001**, *36*, 4995.
   DOI: 10.1023/A: 1011885631876
7. Kiiko V.S.; Makurin Y.N.; Safronov A. A.; *Refract. Ind. Ceram.,* **2003**, *44*, 94.
   DOI: 10.1023/A: 1024763127088
8. Nagabhushana K. R.; Lakshminarasappa B. N.; Singh F.; *Bull. Mater. Sci.,* **2009**, *32*, 515.
   DOI: 10.1007/s12034-009-0076-y
9. Pakrashi S.; Dalai S.; Sabat D.; Singh S.; Chandrasekaran N.; Mukherjee A.;*Chem. Res. Toxicol.* **2011**, *24*, 1899.
   DOI: 10.1021/tx200244g
10. Sherikar B.N.; Umarji A.N.; *Inter. J. Rea. Engg. Technol.,* IC-RICE Conference Issue, **2013**, 434.
    DOI: 10.15623/ijret.2013.0213082
11. Ling H.; Chen W. Y. Y.; Yen F.S.; Huang C.Y.; *Nano Struct. Mater.,* **1999**, *11*, 89.
    DOI: 10.1016/S0965-9773(99)00022-7
12. Zhuravlev V. D.; Bamburov V. G.; Beketov A. R.; Grigorov G.; *Ceramic International,* **2013**, *39*, 1379.
    DOI: 10.1016/j.mseb.2004.03.024
13. Wang W. N.; Itoh Y.; Lenggoro I. W.; Okuyama K.; *Mater. Sci. Engg. B.,* **2004**, *111*, 69.
    DOI: 10.1016/j.mseb.2004.03.024
14. Rao K. V.; Sunandana C. S.; *J. Nanosci. Nanotechnol.,* **2008**, *8*, 4247.
    DOI: 10.1166/jnn.2008.AN59
15. Patil K.C.; Aruna S.T.; Mimani T.; *Curr. Opin. Solid Stat Mater. Sci.*, **2002**, *6*, 507.
    DOI: 10.1016/S1359-0286(02)00123-7
16. Raveendra R. S.; Prashanth P. A.; Krishna R. H.; Bhagya N. P.; Nagabhushana B. M.; Naika H. R.; Lingaraju K.; Nagabhushana H.; Prasad B. D.; *J. Asian Ceram. Soc.,* **2014**, *2*, 357.
    DOI: 10.1016/j.jascer.2014.07.008
17. Prashanth P. A.; Raveendra R. S.; Krishna R. H.; Bhagya N. P.; Ananda S.; Nagabhushana B. M.; Lingaraju K.; Naika H. R.; *J. Asian Ceram. Soc.,* **2015**, *3*, 345.
    DOI: 10.1016/j.jascer.2015.07.001
18. Ramesh G.; Mangalaraja R. V.; kumar S. A.; Manohar P.; *Int. J. Phys. Sci.,* **2013**, *8*, 1729.
    DOI: 10.5897/IJPS2013.3988
19. Dynys F. W.; Halloran J. W.; *J. Am Ceram Soc.,* **1982**, *65*, 442.
    DOI: 10.1111/j.1151-2916.1982.tb10511.x
20. Klug P.; Alexander L. E.; (Eds) *X-ray Diffraction Procedure*. Wiley; New York, **1954**.
    DOI: 10.1002/pol.1955.120178412